



PERGAMON

Journal of Geodynamics 36 (2003) 51–66

JOURNAL OF
GEODYNAMICS

www.elsevier.com/locate/jog

The Gubbio fault: can different methods give pictures of the same object?

C. Collettini^{a,*}, M.R. Barchi^a, L. Chiaraluce^{a,b}, F. Mirabella^a, S. Pucci^b

^a*Dipartimento di Scienze della Terra Università degli Studi di Perugia, Piazza dell'Università 1, 06100, Perugia, Italy*

^b*Istituto Nazionale di Geofisica e Vulcanologia, Dipartimento di Sismologia e Tettonofisica, Via di Vigna Murata, 605, 00143, Roma, Italy*

Abstract

Different investigation techniques (field geology and structural analysis, geomorphology, seismic reflection profiles and seismological data) have been used to develop images of the Gubbio fault, giving us the opportunity to compare different approaches and evaluate points of consensus and controversy in fault analysis and characterization. From our integrated analysis we define a well-focussed image of the geometry and kinematics of the Gubbio fault and the related Quaternary basin, while the seismogenic role of the fault is still ambiguous.

© 2003 Elsevier Ltd. All rights reserved.

1. Introduction

Different methods of investigation using well-established techniques are commonly used in fault analysis. A geologist looks for sudden changes in lithology, describes the fault plane characteristics and the associated fault rocks and performs geometric and kinematic analysis. A geomorphologist studies irregularities in slopes and anomalies in the drainage network linked with faulting. A geophysicist searches for a prominent reflector on a seismic profile and/or interruption and displacement of stratigraphic seismic markers. A seismologist focuses on the assessment of seismic energy release associated with earthquakes nucleated along specific faults and on the kinematic of the rupture, as well as on the geometry and distribution properties of aftershock sequences. Each method of investigation provides its own picture of a fault; the comparison and integration of these different methods, however, is not a trivial matter.

* Corresponding author. Tel.: +39-075-5852651; fax: +39-075-585260.

E-mail address: colle@unipg.it (C. Collettini).

In this paper we discuss this problem in detail in order to emphasise the importance of a multidisciplinary approach for the study of active faults. To this aim, we refer to the Gubbio normal Fault, GuF, located in the northern Apennines of Italy. This structure gives us the opportunity of comparing different available data sets, such as: (i) updated geological and geomorphological information on both the fault and the associated basin area, (ii) good quality seismic reflection profiles, and (iii) seismological data recorded during the 1984 seismic sequence.

The northern Apennines are characterised by the presence of a complex pattern of thrusts, folds and normal faults, reflecting the superposition of two main tectonic phases: an upper Miocene–lower Pliocene compressional phase, forming E–NE verging thrusts and folds, and a superimposed, upper Pliocene–Quaternary extensional phase, forming extensional basins bounded by

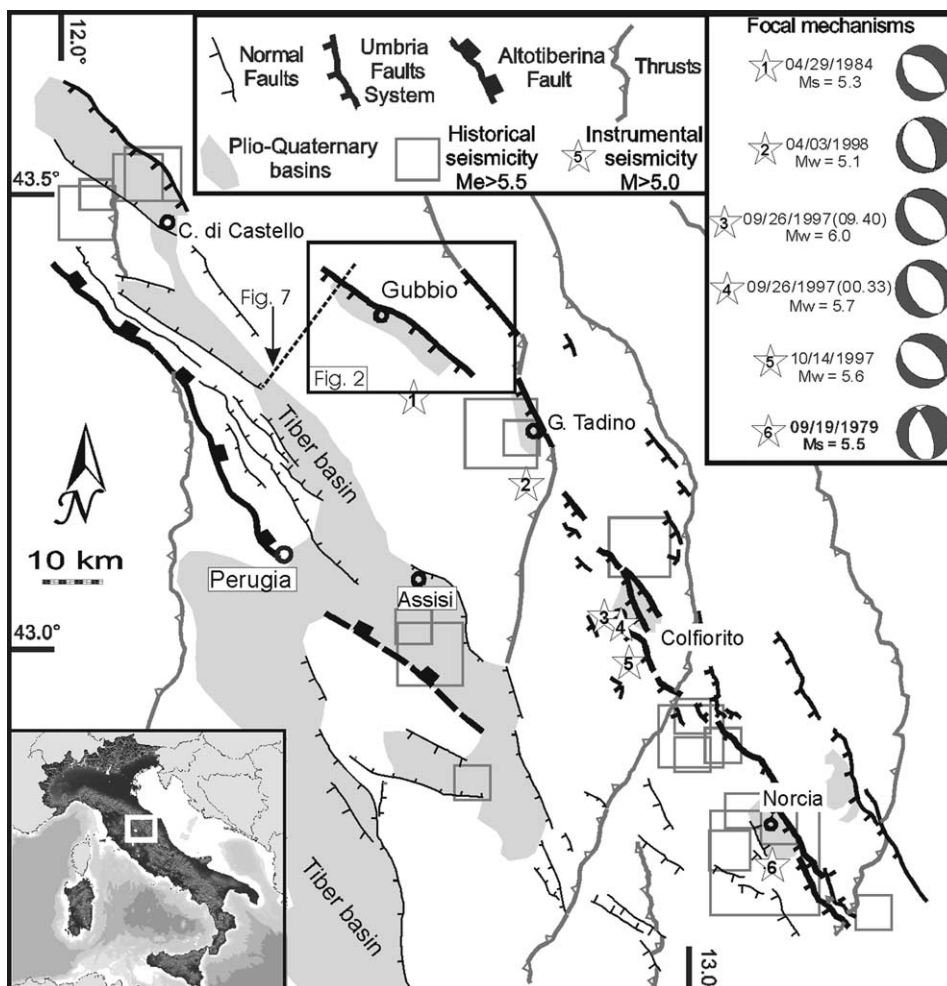


Fig. 1. Schematic Structural map of Umbria showing the alignment of the intramountain basins along the Umbrian Fault System, UFS. Historical seismicity is reported for the period 461 BC–1979 AD (Boschi et al., 1997). Focal mechanisms and magnitudes are for the 1997–1998 Colfiorito sequence (Ekström et al., 1998), for the 1979 Norcia earthquake (Deschamps et al., 1984), and for the 1984 Gubbio earthquake (Dziewonski et al., 1985).

NNW–SSE trending normal faults. Within the northern Apennines the Umbria region is affected by a 150 km long alignment of NNW–SSE trending, SW-dipping active normal faults (Umbria Fault System UFS), where the strongest historical and instrumental seismicity (Intensity = XI; $5 < M < 6$) occurs (Boschi et al., 1997; Barchi et al., 2000 and references therein). The Gubbio fault is a segment of this active alignment (Fig. 1) and the area was affected in 1984, by moderate instrumental seismicity associated to the Gubbio earthquake: $M_s = 5.2$ (Haessler et al., 1988).

In the following paragraphs we illustrate data from surface geology, structural analysis, geomorphology, seismic reflection profiles and seismology, and then propose a discussion about the possibility of integrating different data sources into a coherent image of the GuF.

2. Surface geology and structural data

The geological map of Fig. 2 shows the NNW–SSE trending Gubbio normal fault cutting and downthrowing the backlimb of a pre-existing, NE verging anticline. In the NW portion of the GuF, the footwall is made of the Jurassic-Oligocene carbonatic succession of the Umbria-Marche Apennines, which form the culmination of the anticline. In the SW portion of the GuF, the

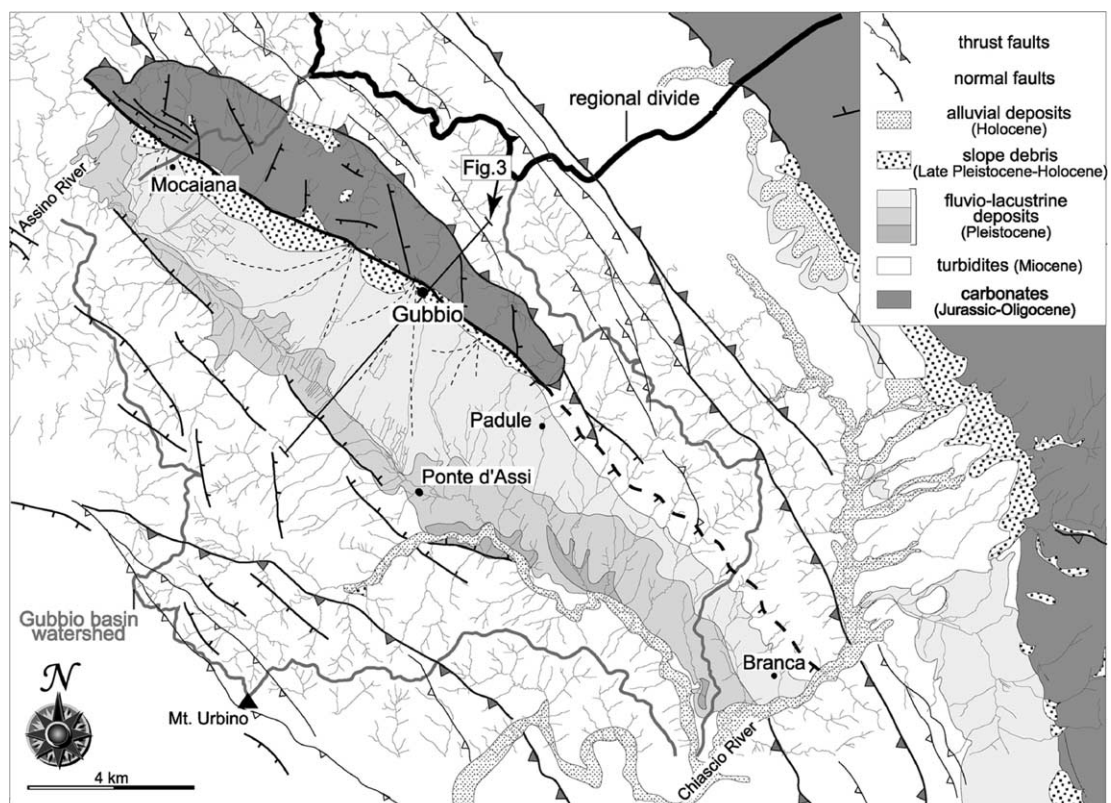


Fig. 2. Simplified map of the Gubbio area modified after Bonarelli et al. (1952), Moretti and Perno (1968), Menichetti (1992), showing the drainage network of the Gubbio basin and its watershed.

footwall is made of the Miocene turbidites of the Marnoso-Arenacea fm. In the hangingwall, the Quaternary Gubbio basin is infilled with fluvio-lacustrine deposits, consisting of three units, from bottom to top: a clayey lignitic basal complex, a clayey sandy complex and an alluvial complex (GE.MI.NA., 1963; Pucci et al., in press). The basin has a longitudinal length of 22 km and a maximum width of 4 km. The southern termination is quite sharp and corresponds to a SW–NE, lineament including a segment of the Chiascio river valley (Cencetti, 1988). The exposure, in the south-western part of the basin, of gently NE-dipping lignite beds, pertaining to the lower units of the fluvio-lacustrine deposits, highlights the asymmetric geometry of the basin which shows an overall triangle shape (Fig. 3) and a maximum thickness of ~400 m in proximity of the GuF (Menichetti, 1992).

Structural analysis of the Gubbio fault shows that the associated deformation zone (up to 150 m wide) consists of synthetic and subordinate antithetic splays showing Andersonian dips, $52^\circ < \delta < 78^\circ$, and a slightly bimodal strike direction (azimuth $120\text{--}140^\circ$); all these features display a close to pure dip-slip kinematics (Fig. 4a). Extensional deformation in the exposed footwall block is characterised by conjugate systems of normal mesoscopic faults (Fig. 3c), trending parallel to the GuF (Fig. 4b). Their dip distribution is in the $30\text{--}90^\circ$ range with a peak for Andersonian values. Striated fault planes were analysed in 16 structural stations, homogeneously distributed within the study area; inversion of slip data for each population of faults was computed by a standard inversion technique (DAISY, Salvini, 1998), and the results allowed us to define a constant stress tensor with a vertical σ_1 and a SW–NE oriented σ_3 (Fig. 4c). This stress

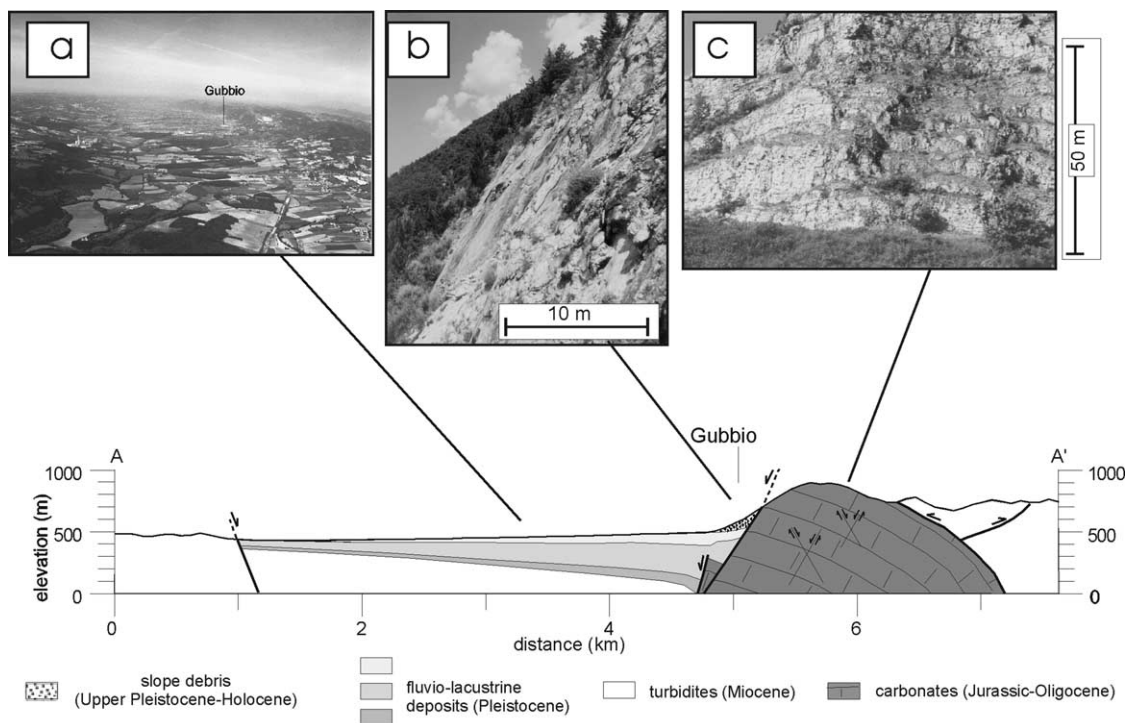


Fig. 3. Pictures of the Gubbio structure at the surface: (a) Gubbio basin; (b) Gubbio fault plane; (c) Extensional deformation in the footwall block.

tensor is similar to that obtained from other local and regional studies in this sector of the Apennines (e.g. Lavecchia et al., 1994; Boncio et al., 1996, 2000).

3. Geomorphology

A set of topographic profiles through the Gubbio basin shows that the basin floor lies at about 400 m a.s.l., whereas the eastern and western ranges reach elevations of about 950 and 650 m a.s.l. respectively (Fig. 5).

The eastern flank of the basin shows the highest elevation and steepest slopes, with relevant debris deposition. Sinuosity of the mountain–piedmont contact is quite high (Fig. 5), hence suggesting that

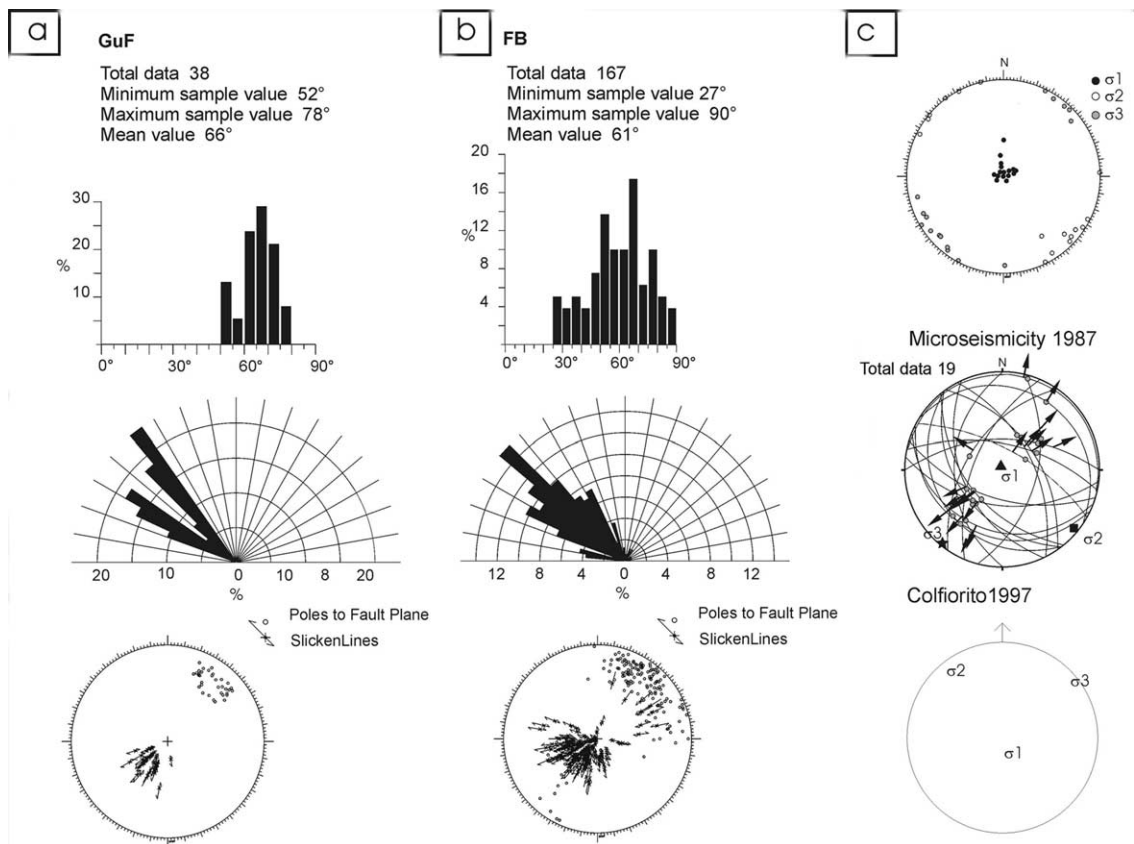


Fig. 4. Extensional deformation structural analysis: (a) Gubbio normal fault dip, strike and stereoplot (Schmidt equal area projection, lower hemisphere); (b) footwall normal fault dip, strike and stereoplot (Schmidt equal area projection, lower hemisphere); (c) stress tensor analyses from top to bottom: reconstruction of the stress tensor at each structural station, reconstruction of the stress tensor (Boncio et al., 1996) by using microseismicity recorded in the study area (1987 microseismic survey, Deschamps et al., 1989), reconstruction of the stress tensor by using the six mainshocks of the Colfiorito 1997 seismic sequence (Chiarioluca et al., in press).

slope evolution was controlled by low activity faults (e.g. Bull and McFadden, 1977). The northern sector (Fig. 6) shows a typical regularised slope replacement profile (e.g. Bartolini, 1992) with a constant inclination of about 30° (Section 1 and 2 in Fig. 6). The surface slope of these deposits is higher than their depositional dip (about 15°), thus indicating that its dynamic development was influenced by a strong erosional activity. This can either be interpreted as due to the lowering of the local base level or to a regional tectonic uplift. The southern sector exhibits higher

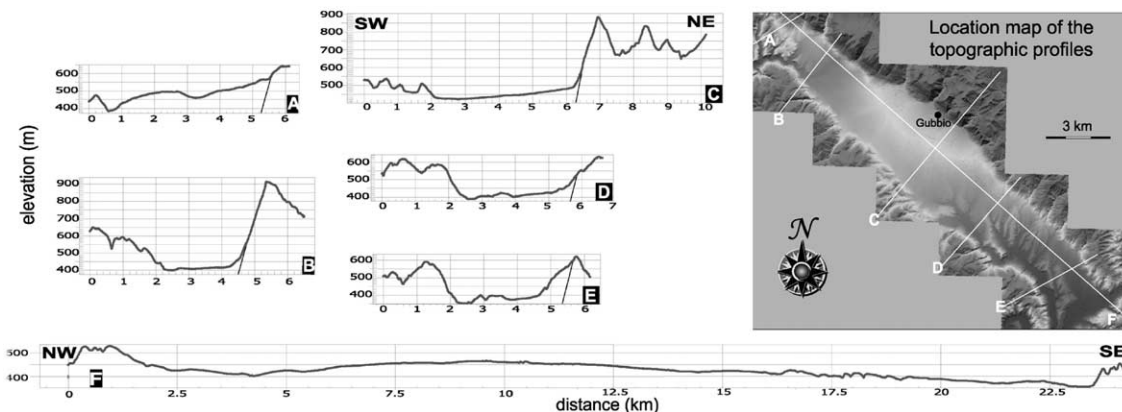


Fig. 5. Topographic profiles across and parallel to the Gubbio basin performed by means of 5-m resolution DEM. The position of the Gubbio fault trace is shown in the profiles.

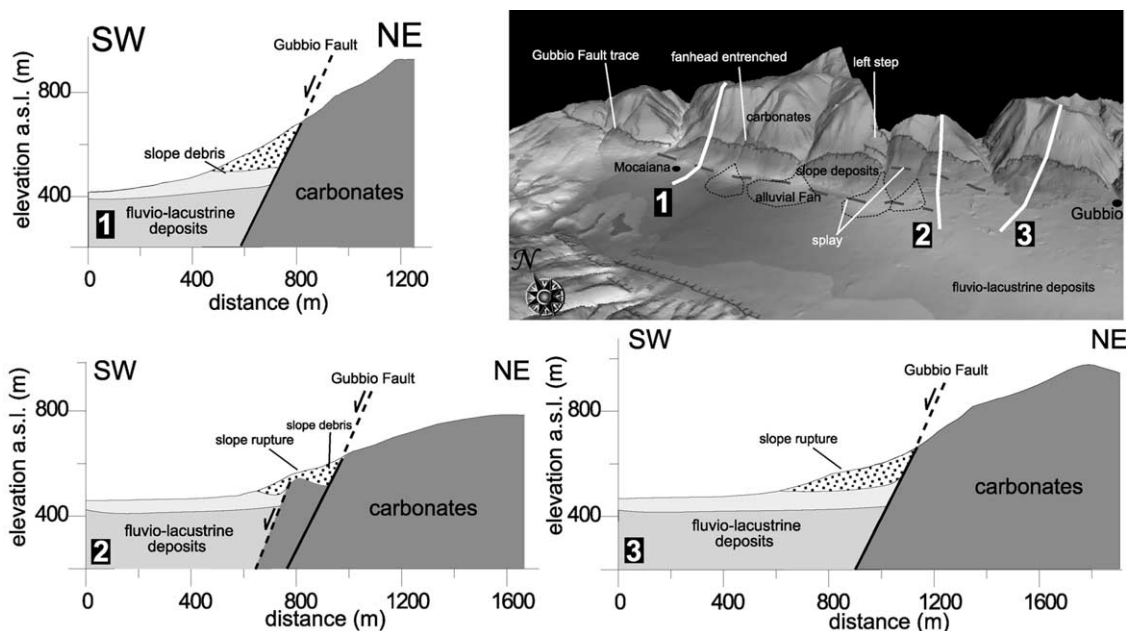


Fig. 6. Detailed topographic profiles across the carbonatic portion of the Gubbio anticline. Slope profile with a constant inclination of about 30° (Section 1). Higher inclination in the southern part (35° Section 3, Fig. 6).

inclinations (35° ; see Section 3 in Fig. 6) which are almost equal to the depositional dips: the topographic profiles show irregularities and morphologic scarps within the slope debris (e.g. Section 2 in Fig. 6). Left oversteps of the GuF are exposed between Gubbio and Mocaiana, where the slope debris has the largest surface extension and reaches the highest elevations within the basin. The presence of several slope ruptures within the debris, which are mostly rectilinear and aligned for a maximum length of 2 km, suggests the existence of at least two main fault splays below the continental deposits (Fig. 6).

The western flank of the basin has a completely different morphologic expression with respect to the eastern one, and lower relief energy. The mountain–piedmont junction is noticeably dissected and the slope shows clear straight NNW–SSE trending lineaments, typical of fault-controlled slopes (see DEM in Fig. 5). Two main NNW–SSE trending tectonic lineaments, mapped in detail for more than 15 km, have been recognised along this flank of the basin (Pucci et al., *in press*) showing paleosurface outeredges and aligned scarps in colluvium and bedrock.

As concerns the drainage of the Gubbio basin, it consists of two secondary hydrographic networks connected with the Assino river to the north and Chiascio river to the south. A system of alluvial fans, centred close to the town of Gubbio, acts as a local water divide within the basin: the northern creek, tributary of the Assino River, and the southern creek, tributary of the Chiascio River, flow in opposite directions across the Pleistocene deposits (Fig. 2). The main southern creek is linear, flows parallel to the maximum basin elongation, and is located close to its western flank. This asymmetry may be explained with a westward progressive migration of the rivers as the alluvial fans prograded; however, the permanence of the creek, where large alluvial fans are not present, also suggests a tectonic control.

In conclusion, it is difficult to identify clear recent geomorphological evidence of the GuF in the eastern flank of the Gubbio basin. This is possibly linked to the prevalence of erosional processes on tectonics. The geomorphic analysis also suggests the presence of NE-dipping, possibly active normal faults, antithetic to the GuF, and bounding the western margin of the basin.

4. Seismic reflection profiles

The subsurface setting of the Gubbio area has been studied by interpreting and converting to depth a set of 6, good quality, commercial seismic reflection profiles trending roughly perpendicular to the GuF. The interpretation of this data set is shown in Pauselli et al. (2002) and Mirabella (2002). The stratigraphy of the area consists schematically of four major lithological units, from top to bottom: Miocene turbidites, Jurassic-Oligocene carbonates, Triassic evaporites, Paleozoic-Triassic phyllitic basement. The seismic profiles show at least four main seismic markers, calibrated with borehole data (Bally et al., 1986; Anelli et al., 1994); they correspond to the: Bisciario Fm. (resting at the base of the Miocene turbidites), Marne a Fucoidi Fm. (a marly interval within a prevalently carbonatic sequence), the top of Triassic evaporites and the top of the phyllitic basement. These seismic markers can easily be traced throughout the region.

Seismic images show that the backlimb of the Gubbio anticline is displaced and downthrown by the GuF (Fig. 7). The fault geometry at depth is represented by the alignment of W-dipping reflections and by the strong interruption and displacement of the seismic markers. The fault

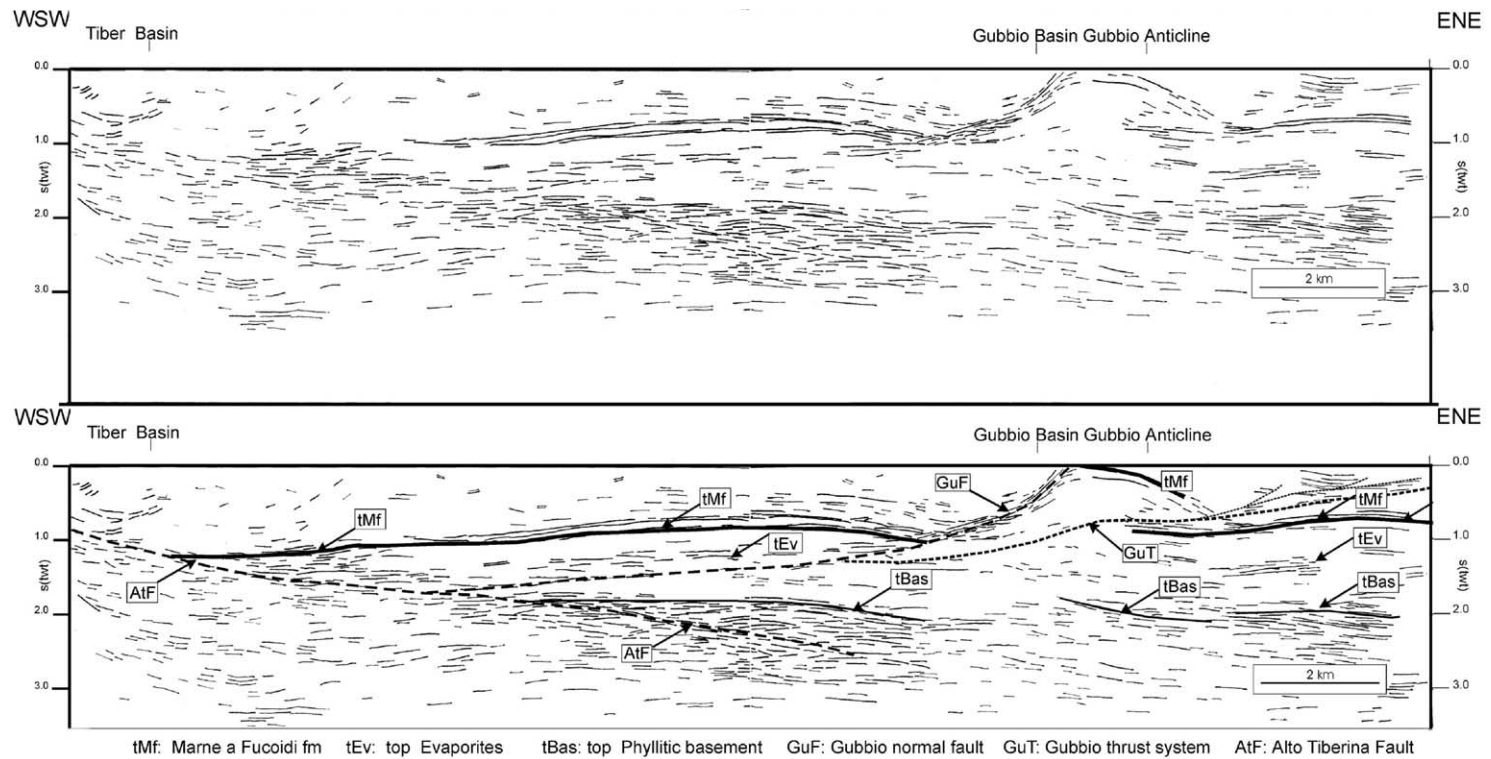


Fig. 7. Seismic reflection profile through the study area, see location in Fig. 1.

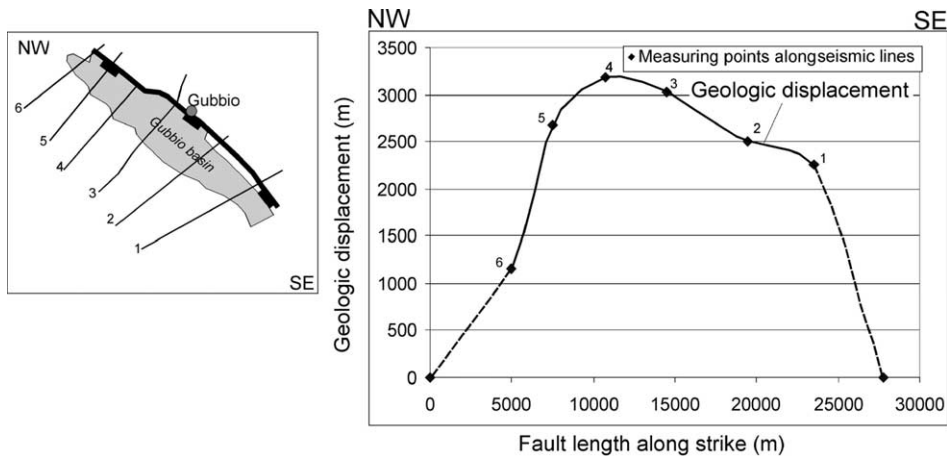


Fig. 8. Variation of the displacement along the GuF strike. The curve has been constructed by using the displacement of the Marne a Fucoidi reflector on seismic profiles. The topographic throw has been constructed using.

geometry is steep in its shallow portion, $\delta \sim 45^\circ$ for the first 4 km, and gently dipping at depth, $\delta \sim 20^\circ$ at 5–6 km; the deeper portion of the fault reactivates a thrust of the previous compressional phase, which formed the Gubbio anticline. The GuF is antithetic and detached on a regional NE-dipping low-angle normal fault, the Altotiberina fault (ATF; Barchi et al., 1999; Boncio et al., 2000; Collettini et al., 2000) which bounds the westernmost Tiber basin at the surface (Fig. 1).

Displacement variations along the GuF have been assessed by using the Marne a Fucoidi reflector (Fig. 8): displacement data show a bell-shaped geometry and maximum displacement value (~ 3.2 km) at the centre of the Gubbio Quaternary basin.

5. Seismological data

In the last two decades, three seismic sequences have been recorded in the Central Apennines at: Norcia 1979 $M_w = 5.8$, Gubbio 1984 $M_w = 5.6$ and Colfiorito 1997–1998 $M_w < 6.0$ (Deschamps et al., 1984; Haessler et al., 1988; Westaway et al., 1989; Amato et al., 1998). Improved techniques in earthquake recording and location have led to high resolution definition of the Colfiorito sequence only (Chiaraluce et al., in press), whereas earlier seismic sequences are less well defined.

On 29 April 1984, the Gubbio area was struck by an earthquake, $M_s = 5.2$ (Haessler et al., 1988). Because good permanent station coverage was lacking and a temporary seismic network was installed only three days after the event, a poorly constrained data set was obtained for: location of the mainshock, focal mechanism solution and aftershock distribution (Fig. 9).

We relocated with the “double-difference” relocation algorithm (Waldhauser and Ellsworth, 2000) the ~ 300 aftershocks ($M < 3.5$), recorded within a week at a temporary, local network of

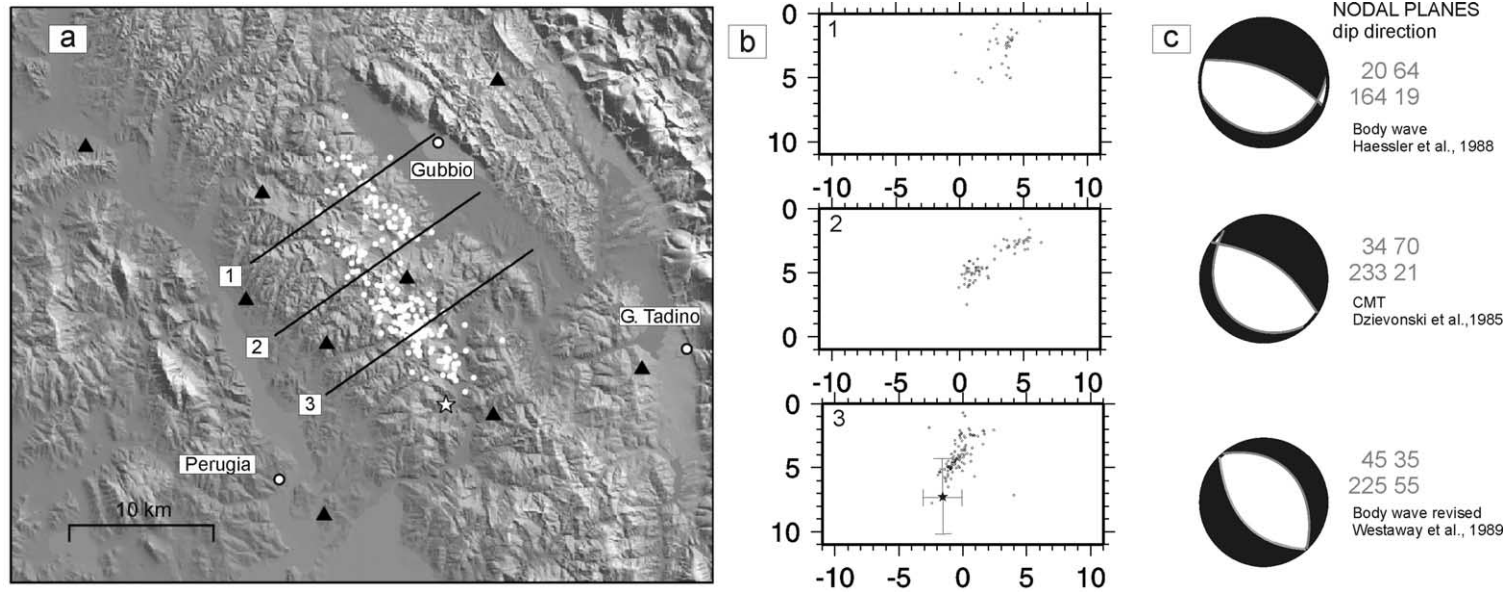


Fig. 9. Seismological data of the 1984 seismic sequence: (a) map of mainshock and aftershock distribution; (b) mainshock and aftershock distribution cross sections; (c) focal mechanisms available for the same mainshock: (1) body wave focal mechanisms (Haessler et al., 1988); (2) CMT (Dziewonski et al., 1985); (3) revised body wave focal mechanism (Westaway et al., 1989).

Table 1
Velocity model for the location of the aftershocks and mainshock

Depth (km)	v (km/s)
<i>(a) Aftershocks</i>	
0	4
1.5	5
5	5.6
8	6
34	8
<i>(b) Mainshocks</i>	
0	5
11	6.5
38	8.5

nine stations. We used a 1D velocity model (Table 1a) derived from geological information, a V_p/V_s ratio of 1.85 (Haessler et al., 1988) and at least six P-phases for each earthquake. The final data (Fig. 9) consist of 215 relocated events, with mean RMS of 0.04 s and formal horizontal and vertical errors of 200 and 400 m, respectively. The general shape of the seismicity on the map is very similar to that presented by Haessler et al. (1988). The elongation of the seismicity in the N130E direction and the two sub-parallel linear clusters are still evident. Differences can be found in the seismicity distribution at depth, where our locations are slightly shallower with most of the seismicity located between 1 and 6 km. In the northern cluster (10 km long and 3 km wide) seismicity is mainly confined between 1 and 4 km, whereas in the southern cluster (14 km long and 5 km wide) it is confined within 4 and 6 km. The registered aftershocks are systematically distributed in the GuF hangingwall and suggest a SW dipping plane as the most likely ruptured fault. However the distribution does not unambiguously define a fault plane. This can be explained considering the experience of Colfiorito (another active segment of the UFS), where the on-fault aftershocks nucleated in the first few hours following the main shock (Chiaraluce et al., submitted for publication). This kind of information for Gubbio is lacking, because the local network was installed 3 days after the mainshock.

Even more ambiguous is the location of the main shock: we recomputed available data by using the Hypoinverse code (Klein, 1978) and a simple regional velocity model derived from the Italian National Network of the INGV (Table 1b). We used 16 phases recorded at stations within a 350 km radius, thus obtaining a focal depth of ~ 7 km with a final RMS of 0.45 s and a final error of 1.5 and 3.5 km horizontally and vertically respectively. The epicentre of the main shock is located at the SE edge of the larger cluster, hence suggesting that the rupture propagated towards the NNW (Fig. 9a).

The focal mechanism solution associated to the mainshock is very controversial too; three different focal mechanism solutions are available for the same mainshock (Fig. 9c): (1) a body wave focal mechanism (Haessler et al., 1988), (2) a CMT solution (Dziewonski et al., 1985), and (3) a revised body wave focal mechanism (Westaway et al., 1989). The last two solutions show NW–SE trending focal planes that are consistent with the strike of the GuF and of the active faults of the region.

6. Discussion and conclusions

6.1. The GuF: a focused picture

Data illustrated above define a coherent and focused image of the GuF; each method, in fact, contributed, in its own way, to characterise the fault and the associated tectono-sedimentary structures (Fig. 10 and Table 2). From our integrated analysis, we show that: (i) fault length (22 km) and orientation (N130°) strictly correspond to the length and orientation of the Quaternary

Table 2

The GuF pictures of the same object. Images of the GuF from surface geology, geomorphology, seismic reflection profiles and seismological data

	GuF strike	GuF dip (δ)	GuF length	Notes
Surface geology	Azimuth 120–140°	58° < δ < 78°	Fault length 22 km Basin length 22 km	Fault zone up to 150 m wide Small displacement normal fault in the footwall block trending parallel to the GuF Syntectonic basin up to 400 m deep Long term (Quaternary) geological stress tensor with vertical σ_1 and SW-NE oriented σ_3
Geomorphology	Azimuth \sim 130°	Steep fault	Topographic expression 22 km long	Weak evidence of faults cutting Holocene sediments
Seismic reflection profiles	Azimuth \sim 130°	$\delta \sim$ 45° depth 0–4 km, $\delta \sim$ 20° depth 5–6 km	Fault length 22 km	The fault is a prominent reflector Along strike fault displacement, bell-shaped, leading to a high long-term slip rate \sim 1.8 mm/year.
Seismological data	MEQ 1 azimuth 74°	MEQ 1 $\delta = 19^\circ$	Length of the activated area 20 km	Aftershock sequence located in the GuF hangingwall, above the intersection with the ATF
	MEQ 2 azimuth 143°	MEQ 2 $\delta = 21^\circ$		Up-dip migration of the seismicity with time
	MEQ 3 azimuth 135°	MEQ 3 $\delta = 55^\circ$		No clear connection between seismological imaged fault (mainshock and aftershocks) and the seismic profile imaged fault

MEQ = focal mechanisms available in literature for the Gubbio earthquake; the reported azimuth is for an S dipping plane (event 1) and SW-dipping planes (events 2 and 3).

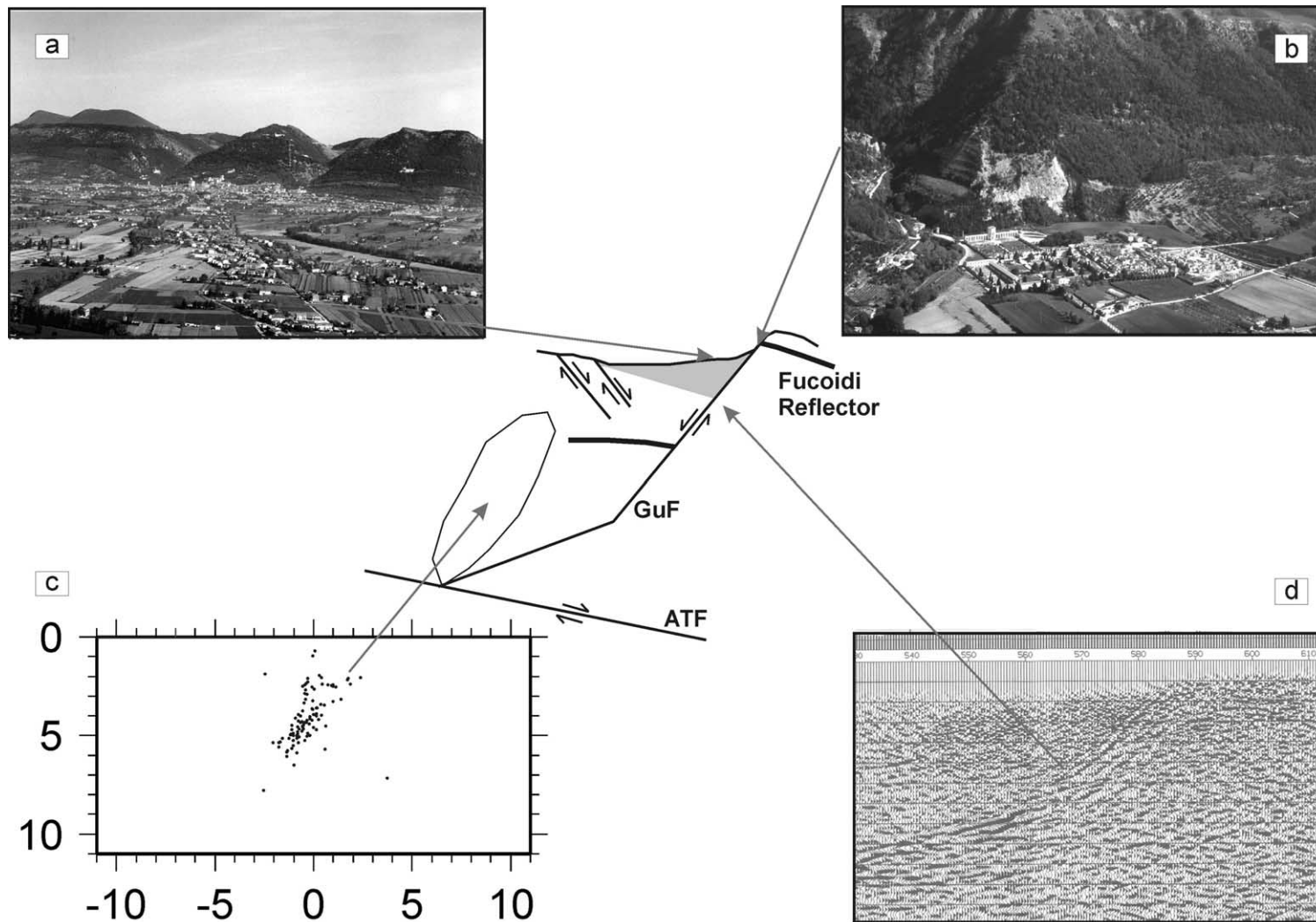


Fig. 10. Cartoon with pictures of the GuF: (a) Gubbio basin and carbonatic anticline; (b) Gubbio fault plane and alluvial fan; (c) aftershock distribution of the 1984 earthquake, (d) seismic image of the GuF.

basin; (ii) the steeply dipping fault plane measured at the surface, $52^\circ < \delta < 78^\circ$, is consistent with the geomorphic expression of the structure and can be easily merged with the seismic image of the shallower portion of the fault trace, dipping about 45° in the first 4 km; (iii) the strong asymmetry of the basin, infilled with syntectonic sediments, is clearly related to the activity of the SW-dipping GuF; (iv) geometric reconstructions, based on the asymmetrical shape of the basin, lead [Menichetti and Minelli \(1991\)](#) to hypothesise a listric geometry with the depth of the basal detachment in the range 6–8 km; the geometry at depth of the GuF, constrained by seismic reflection data, offers a similar picture, showing a gently W-dipping (20°), basal fault at depth ≤ 6 km; (v) maximum displacements across the GuF exceed 2 km, and the observed continuity of the fault trace at the surface, along with the bell-shaped geometry of the displacement curve of [Fig. 8](#), indicate that the GuF consists of a single fault plane. (vi) surface geology and geomorphology highlight the presence of overlapping splays: the width of the overlapping zone (< 500 m) is very low compared to the length of the single fault segments (~ 5 km), thus indicating that this segmentation is a very shallow feature (cf. [Fig. 6](#)); (vii) E-dipping faults (antithetic to the GuF master fault) mapped along the western flank of the basin ([Pucci et al., in press](#)) and more to the west within the Marnoso-Arenacea turbidites ([Menichetti, 1992](#)), display relatively low displacements (~ 200 m, i.e. one order magnitude lower than the GuF) and, according to our interpretation of available seismic lines, appear to be shallow structures which do not offset the top of the carbonates; and (viii) the stress tensor obtained from the inversion of the striated fault planes, i.e. the long-term Quaternary stress field, is constant within the Gubbio area and is consistent with the orientation of both the GuF and the geological stress tensor derived from other Quaternary faults in the region ([Lavecchia et al., 1994](#); [Boncio et al., 1996](#)).

The evaluation of the Quaternary average slip-rate is more difficult to address. The maximum displacement measured through seismic reflection profiles is 2800–3200 m: assuming that all the displacement occurred during the Quaternary (age of the syntectonic sediments), the corresponding average slip-rate would be 1.65–1.9 mm/year, a very high value compared to the slip-rates evaluated for other faults of the UFS (≤ 0.8 mm/year; [Barchi et al., 2000](#)). We cannot exclude that a part of the GuF displacement is associated to pre-Quaternary activity: for example [Tavarnelli and Peacock \(2002\)](#) suggest a pre-orogenic extensional phase, documented also for other normal faults of the Umbria-Marche region (e.g. [Scisciani et al., 2002](#)).

6.2. The seismogenic GuF: an out of focus picture

For what concerns the seismogenic role of the GuF, the available dataset is more controversial. In fact there is little geological and geomorphological evidence of very recent activity of the fault, though this can be explained by erosion prevailing on tectonics. Furthermore, no coseismic surface breaks were observed during the 1984 earthquake and no other instrumental or historical earthquakes are located within the Gubbio area itself.

On the other hand, some evidence supporting a seismogenic role of the GuF can be derived from the following points:

1. The GuF is part of the active alignment of the northern Apennines (UFS, [Fig. 1](#)), and shows the same geometrical and geological characters of the active faults in the area (SW-dipping, Andersonian, basin-bounding normal fault).

2. The stress tensor obtained from the inversion of the striated fault planes is constant within the Gubbio area and is consistent with both the orientation of the GuF and the active stress tensor of the UFS (Boncio et al., 1996; Montone et al., 1999; Chiaraluce et al., in press). The GuF is also favourably oriented for activation within this stress field (Fig. 4c).
3. Two of the three different focal mechanisms available for the mainshock have strikes which are consistent with the direction of the fault and also with the aftershock distribution.

In conclusion we emphasise that the state of the art on the spatial and dimensional properties of the GuF depicts a well-focussed image of this structure, whereas the contrasting information available until now on its role as a seismogenic fault still need to be better focussed, in order to consider more confidently the GuF as an earthquake source in central Italy.

Acknowledgements

Research leading to this paper was supported by MIUR01 UR Perugia and Regione Umbria. We would like to thank ENI-AGIP, particularly S. Merlini, who provided the data set of seismic reflection profiles.

References

- Amato, A., Azzara, R., Chiarabba, C., Cimini, G.B., Cocco, M., Di Bona, M., Margheriti, L., Mazza, S., Mele, F., Selvaggi, G., Basili, A., Boschi, E., Courboux, F., Deschamps, A., Gaffet, S., Bittarelli, G., Chiaraluce, L., Piccinini, D., Ripepe, M., 1998. The 1997 Umbria-Marche, Italy, earthquake sequence: a first look at the main shocks and aftershocks. *Geophysical Research Letters* 25, 2861–2864.
- Anelli, L., Gorza, M., Pieri, M., Riva, M., 1994. Subsurface well data in the Northern Apennines (Italy). *Memorie Società Geologica Italiana* 48, 461–471.
- Bally, A.W., Burbi, L., Cooper, C., Ghelardoni, L., 1986. Balanced sections and seismic reflection profiles across the Central Apennines. *Memorie Società Geologica Italiana* 35, 257–310.
- Barchi, M. R., Galadini, F., Lavecchia, G., Messina, P., Michetti, A. M., Peruzza, L., Pizzi, A., Tondi, E., Vittori, E., 2000. Sintesi sulle conoscenze delle faglie attive in Italia Centrale. Gruppo Nazionale per la Difesa dei Terremoti.
- Barchi, M.R., Paolacci, S., Pauselli, C., Piali, G., Merlini, S., 1999. Geometria delle deformazioni estensionali recenti nel bacino dell'Alta Val Tiberina fra S. Giustino Umbro e Perugia: Evidenze geofisiche e considerazioni geologiche. *Bollettino Società Geologica Italiana* 118, 617–625.
- Bartolini, C., 1992. I fattori geologici delle forme del rilievo. Pitagora, Bologna.
- Bonarelli, G., Lipparini, T., Moretti, A., Pillotti, C., Principi, P., Scarsella, F., Selli, R., 1952. Carta geologica d'Italia 1:100000 (1st ed.)—sheet 116, Gubbio, Italian Geological Survey.
- Boncio, P., Brozzetti, F., Lavecchia, G., 1996. State of stress in the Northern Umbria-Marche Apennines (Central Italy): inferences from microearthquake and fault kinematic analyses. *Annales Tectonicae* 10 (1–2), 80–97.
- Boncio, P., Brozzetti, F., Lavecchia, G., 2000. Architecture and seismotectonics of a regional low-angle normal fault zone in Central Italy. *Tectonics* 19 (6), 1038–1055.
- Boschi, E., Guidoboni, E., Ferrari, G., Valensise, G., Gasperini, P., 1997. CFTI, Catalogo dei Forti Terremoti Italiani dal 461 a.C. al 1990. Istituto Nazionale di Geofisica, Storia Geofisica Ambiente, Bologna.
- Bull, W.B., Mc Fadden, L.D., 1977. Tectonic geomorphology north and south of the Garlock Fault, California. In: Doehring, D.O. (Ed.), *Geomorphology in Arid Regions*. State University of New York at Binghamton, Binghamton, NY, pp. 115–138.

- Cencetti, C., 1988. Evoluzione del reticolo idrografico in un tratto umbro-marchigiano dello spartiacque principale dell'Appennino. *Geogr. Fis. Dinam. Quat.* 11, 11–24.
- Chiaraluce, L., Ellsworth, W.L., Chiarabba, C., Cocco, M. Imaging the complexity of an active complex normal fault system: the 1997 Colfiorito (central Italy) case study. *Journal of Geophysical Research* (in press).
- Collettini, C., Barchi, M.R., Pauselli, C., Federico, C., Piali, G., 2000. Seismic expression of active extensional faults in northern Umbria (central Italy). In: Cello G., Tondi E. (eds.) *The Resolution of Geological Analysis and Models for Earthquake Faulting Studies*. *Journal of Geodynamics*, 29, 309–321.
- Deschamps, A., Iannaccone, G., Scarpa, R., 1984. The umbrian earthquake (Italy) of 19 september 1979. *Annales Geophysicae* 2 (1), 29–36.
- Deschamps, A., Scarpa, R., Selvaggi, G., 1989. Analisi sismologica del settore settentrionale dell'Appennino umbro-marchigiano. *GNGTS 8th Conference* 1, 9–15.
- Dziewonski, A.M., Franzen, J.E., Woodhouse, J.H., 1985. Centroid-moment tensor solutions for April-June, 1984. *Physics Earth Planetary International* 37, 87–96.
- Ekström, G., Morelli, A., Boschi, E., Dziewonski, A., 1998. Moment tensor analysis of the Central Italy earthquake sequence of september-october 1997. *Geophysical Research Letters* 25 (11), 1971–1974.
- GE.MI.NA (1963): *Ligniti e torbe dell'Italia Centrale*, GE.MI.NA., Geomineraria Nazionale, Torino (publ).
- Haessler, H., Gaulon, R., Rivera, L., Console, R., Frongneux, M., Gasparini, G., Martel, L., Patau, G., Siciliano, M., Cisternas, A., 1988. The Perugia (Italy) earthquake of 29, April 1984: a microearthquake survey. *Bulletin Seismological Society of America* 78, 1948–1964.
- Klein, F.W., 1978. Hypoinverse: user guide to version 1, 2, 3, and 4, US Geol. Surv., Open-File Rept. 78, 694.
- Lavecchia, G., Brozzetti, F., Barchi, M.R., Menichetti, M., Keller, J.V.A., 1994. Seismotectonic zoning in east-central Italy deduced from an analysis of the Neogene to present deformations and related stress fields. *Geological Society of America Bulletin* 106, 1107–1120.
- Menichetti, M., Minelli, G., 1991. Extensional tectonics and seismogenesis in Umbria (Central Italy) the Gubbio area. *Bollettino Società Geologica Italiana* 110, 857–880.
- Menichetti, M., 1992. Evoluzione tettonico-sedimentaria della valle di Gubbio. *Studi Geologici Camerti*, Vol. Spec. 1992/1, 155–163.
- Mirabella, F., 2002. Seismogenesis of the Umbria-Marche Region (Central Italy): Geometry and Kinematics of the Active Faults and Mechanical Behaviour of the Involved Rocks. PhD thesis, University of Perugia (Italy).
- Montone, P., Amato, A., Pondrelli, S., 1999. Active stress map of Italy. *Journal of Geophysical Research* 104, 25595–25610.
- Moretti, A., Perno, U., 1968. *Carta geologica d'Italia 1:100.000* (2nd ed.)—sheet 123, Assisi, Italian Geological Survey.
- Pauselli, C., Marchesi, R., Barchi, M.R., 2002. Seismic image of the compressional and extensional structures in the Gubbio area (Umbria-Pre Apennines). *Bollettino Società Geologica Italiana*, Vol. Spec 1, 263–272.
- Pucci, S., De Martini, P.M., Pantosti D., Valensise, G. Geomorphology of the Gubbio basin (Central Italy): understanding the active tectonics and earthquake potential. *Annals of Geophysics* (in press).
- Salvini, F. 1998. *DAISY 2.1 Software*. Rome.
- Scisciani, V., Tavarnelli, E., Calamita, F., Paltrinieri, W., 2002. Pre-thrusting normal faults within syn-orogenic basins of the Outer Central Apennines, Italy: implication for Apennine tectonics. *Bollettino Società Geologica Italiana*, Vol. Spec 1, 295–304.
- Tavarnelli, E., Peacock, D.C.P., 2002. Pre-thrusting extension in a syn-orogenic foredeep basin of the Umbria-Marche Apennines, Italy. *Bollettino Società Geologica Italiana*, Vol. Spec 1, 729–737.
- Waldhauser, F., Ellsworth, W.L., 2000. A double-difference earthquake location algorithm: method and application to the northern Hayward Fault, California. *Bulletin Seismological Society of America* 90, 1353–1368.
- Westaway, R., Gawthorpe, R., Tozzi, M., 1989. Seismological and field observations of the 1984 Lazio-Abruzzo earthquakes: implications for the active tectonics of Italy. *Geophysical Journal International* 98, 489–514.